

# Isobutrin from *Butea Monosperma* (Flame of the Forest): A Promising New Natural Sensitizer Belonging to Chalcone Class

Shruti A. Agarkar,<sup>\*,†</sup> Roshan R. Kulkarni,<sup>‡</sup> Vivek V. Dhas,<sup>†</sup> Ashish A. Chinchansure,<sup>‡</sup> Partha Hazra,<sup>§</sup> Swati P. Joshi,<sup>\*,‡</sup> and Satishchandra B. Ogale<sup>\*,†,§</sup>

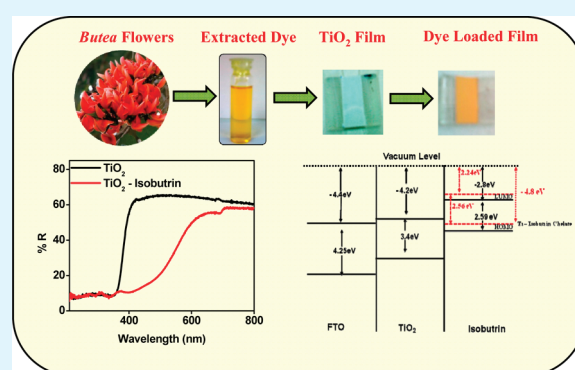
<sup>†</sup>Physical and Materials Chemistry Division and <sup>‡</sup>Organic Chemistry Division, National Chemical Laboratory (Council of Scientific and Industrial Research), Pune 411008, India

<sup>§</sup>Indian Institute of Science Education and Research, Pune 411008, India

**S** Supporting Information

**ABSTRACT:** In this work, “isobutrin”, an ecofriendly sensitizer that is extracted from *Butea monosperma* (commonly known as “Flame of the Forest”) flowers, is introduced. It is a bright yellow pigment belonging to the chalcone class and is examined as a sensitizer for optoelectronic applications. It is observed that chelation of this dye with Ti ions results into a strong dye-TiO<sub>2</sub> charge transfer (DTCT) band in the visible region. This Ti-Isobutrin chelate is stable, irreversible and its formation is studied using Benesi–Hildebrand plot. The locations of HOMO–LUMO states of the Ti-isobutrin chelate and the corresponding band alignment with TiO<sub>2</sub> are obtained. Also, a thermal stability test revealed that isobutrin is stable above 100 °C.

**KEYWORDS:** isobutrin, *Butea monosperma*, chalcone, sensitizer, dye-sensitized solar cell, TiO<sub>2</sub>



## 1. INTRODUCTION

Solar energy is the most abundant, clean and green source of renewable energy and it can be harnessed via different routes in the interest of diverse applications. In many applications such as dye-sensitized solar cells (DSSCs), photocatalysis, solar-to-chemical conversion, etc., sensitizers with good optical properties over the visible range are essential.<sup>1</sup> Although a number of molecular sensitizers in the form of organic dyes (including heavy metal ion incorporated ones) have been synthesized and are being used, the corresponding methods of synthesis, application and prolonged use are not eco-friendly. It is therefore highly desirable to explore sources of new natural dye systems that are stable, nontoxic (biocompatible), and with the desirable optoelectronic properties.<sup>2</sup>

In the case of DSSCs a number of factors such as the choice of the photoanode, the dye, the bottom, the counter electrodes, etc., can limit the cell performance,<sup>3</sup> and a quantitatively significant stable electronic anchorage of the dye to the surface of the metal oxide nanostructure (e.g., TiO<sub>2</sub>, ZnO) is a critical factor that determines the cell efficiency.<sup>4</sup> Among the various dyes that have been tested as sensitizers, ruthenium-based dyes have given the highest efficiency of ~11% on the laboratory scale.<sup>5,6</sup> The main advantage of Ru-based dyes is their efficient metal to ligand charge transfer.<sup>4,7</sup> However, their high cost due to complex synthetic procedures as well as environmental hazards posed by the presence of heavy metals invite search for safer and cheaper alternatives.<sup>8</sup> There have been some interesting explorations of natural dyes in the context of the dye-sensitized solar cell

(DSSC) application using pigments obtained from biomaterials such as flowers, fruits and leaves.<sup>9–16</sup> The natural pigments commonly extracted from flowers and fruits are anthocyanins.<sup>9–12</sup> Anthocyanins give colors ranging from red to blue depending on the pH of the medium. The hydroxyl groups present in the anthocyanin molecule help in the binding of this dye to the TiO<sub>2</sub> surface.<sup>9</sup> The maximum efficiency obtained by use of anthocyanins, i.e., juice obtained from *Hibiscus sabdariffa*, is 3.1%.<sup>17</sup> The problem with anthocyanins is that they are pH sensitive, i.e., good binding with TiO<sub>2</sub> occurs only if anthocyanin is present as flavylum ion species (which is stable) at pH around 1 to 3.2, but if pH is increased this ion gets hydrated to form quinoidal bases.<sup>9</sup> These quinoidal compounds are labile and can be transformed into colorless compounds.<sup>18</sup> If pH becomes more acidic <1 then the compound itself is leached out.<sup>19</sup> Maintaining the right pH is nontrivial and at the same time a very crucial step while extracting anthocyanins. They are also thermally unstable.<sup>9</sup> At high temperature the thermal degradation of anthocyanin takes place by loss of glycosyl moieties and  $\alpha$  diketone formation.<sup>20,21</sup> If extracted at a temperature lower than 25 °C, then the issue of solubility of dye arises, which in turn leads to low efficiency of DSSCs.

Porphyrins, which form the structural core of chlorophylls, the natural light harvesters, have also been examined as another class

**Received:** March 18, 2011

**Accepted:** May 24, 2011

**Published:** May 24, 2011

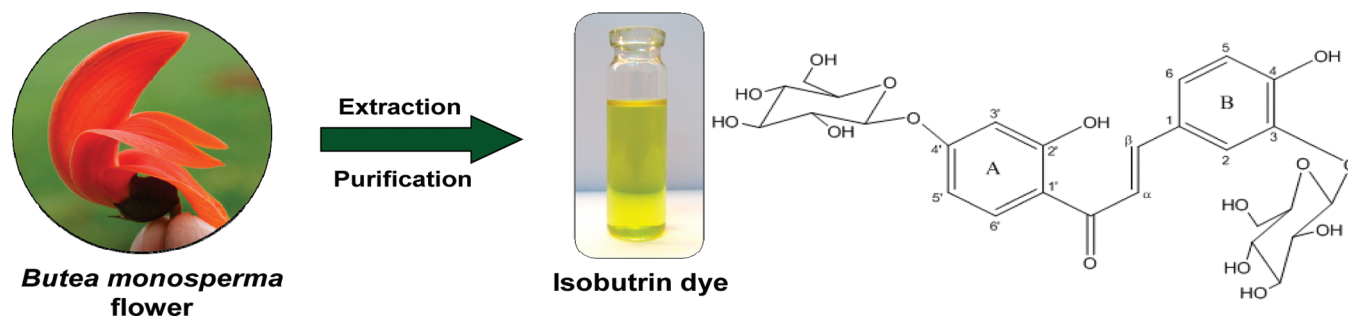


Figure 1. *Butea monosperma* flower, isobutrin dye, and its structure elucidated from  $^1\text{H}$  and  $^{13}\text{C}$  NMR studies.

of sensitizers for DSSCs.<sup>12–15</sup> Campbell et al.<sup>22</sup> have synthesized metal-porphyrin dyes that show conversion efficiency of 7.1%. In 1994, M. Gratzel studied the mechanism of photosensitization of  $\text{TiO}_2$  solar cells by chlorophyll derivatives.<sup>13</sup> In 1986, Kamat and co-workers also explored the use of a chlorophyll analogue as a sensitizer for DSSCs.<sup>14</sup> Natural chlorophyll extracted from Shiso leaves was used as sensitizer by Kumara et al.,<sup>23</sup> which showed efficiency of 0.59%. Isolated chlorophyll was used along with shisosin (an anthocyanin) to realize a synergistic effect that gave efficiency of 1.31%. Betalain pigments extracted from red beet root were also used as dyes which gave efficiency of 0.19%.<sup>24</sup> More recently, Wang and co-workers have done interesting studies on the chlorophyll system and have also modified the dye with metal conjugation to enhance efficiency.<sup>25</sup>

In this work, we introduce a new class of sensitizers, i.e., Chalcones. Chalcones belonging to the flavonoid group are aromatic ketones that form the central core of a variety of important biological compounds, and are known collectively by the said name. They exhibit a broad spectrum of biological activities. *Butea monosperma* (Fabaceae) is a medium sized deciduous tree found in South Asian countries with bright red orange flower clusters. It is commonly called as the “Flame of the Forest” due to its fire like appearance when in full blossom. The flowers of *Butea monosperma* contain various flavonoid compounds such as are butein, isobutrin, butrin, palasitrin, etc., of which isobutrin is one of the major constituents. Isobutrin is a bright yellow colored dye with M.P  $\sim 191$  °C.

## 2. EXPERIMENTAL SECTION

**2.1.  $\text{TiO}_2$  Sphere Synthesis.**  $\text{TiO}_2$  spheres were synthesized following the work of Caruso et al.<sup>26</sup> Transparent  $\text{TiO}_2$ , which was used as bottom layer, was purchased from Solaronix (Switzerland).

**2.2. Characterization of Physical Properties.** The synthesized nanoparticles were characterized using FTIR (Perkin-Elmer Instruments), UV–vis and DRS (Jasco Instruments), Transmission electron microscopy (FEI), and X-ray diffraction (Pan-Analytical).

**2.3. Fabrication and Testing of DSSCs.** To make and study the DSSC solar cells, we employed a doctor blading method. After making the films they were annealed at 450 °C for 30 min. For sensitization, the films were dipped in samples viz juice, separated fraction (aqueous methanol), and isobutrin (5 mM in methanol) for 24 h at room temperature (in separate experiments) and also with 0.5 mM N719 dye in ethanol for comparison. The samples were then rinsed with methanol to remove excess dye on the surface and air-dried at room temperature. This was followed by redox electrolyte addition and top contact of Pt coated FTO. The electrolyte used was 0.6 M 1-propyl-2,3-dimethyl-imidazolium iodide, 0.1 M LiI, 0.05 M  $\text{I}_2$ , and 0.5 M 4-tert-butylpyridine in acetonitrile.<sup>27</sup> The I–V characteristics were measured

under exposure with 100  $\text{mW}/\text{cm}^2$  (450W xenon lamp, Newport Instruments), 1 sun AM 1.5, simulated sunlight as a solar simulator. The current was measured using a Keithley 2400 source. Measurements of the incident-photon-to-current conversion efficiency (IPCE) were performed by changing the excitation wavelength (Newport Instruments). In one set of experiments, the cells were heated to different temperatures up to 200 °C for 1/2 h and their efficiency was tested after cooling to the room temperature (for thermal stability of the dye).

**2.4. Characterization of the Sensitizer.** The  $^1\text{H}$ ,  $^{13}\text{C}$  NMR and DEPT spectra were recorded on Bruker-AV 400 spectrometer operating at 400 and 100 MHz, respectively, in methanol- $d_4$  (Sigma-Aldrich) using TMS as the internal standard. The chemical shift values are reported in ppm ( $\delta$ ) units and the coupling constants ( $J$ ) are in Hz. ESI-MS was recorded on API-QSTAR-PULSAR mass spectrometer. The extract was subjected to column chromatography using silica gel (Spectrochem, India) having a 100–200 mesh size. All solvents were distilled prior to use. Isobutrin structure was confirmed by comparison of its physical constants and spectral properties ( $^1\text{H}$  and  $^{13}\text{C}$  NMR and mass spectroscopy) with those reported in the literature.

Isobutrin: Yellow crystals (mp 191 °C).  $^1\text{H}$  NMR (400 MHz, methanol- $d_4$ ,  $\delta$ ): 7.99 (d,  $J = 8.39$  Hz, 1H; 6'-H), 7.71 (d,  $J = 14.9$  Hz, 1H;  $\beta$ -H), 7.61 (d,  $J = 1.55$  Hz, 1H; 2-H), 7.55 (d,  $J = 14.9$  Hz, 1H,  $\alpha$ -H), 7.27 (dd,  $J = 8.19, 1.55$  Hz, 1H; 6-H), 6.83 (d,  $J = 8.19$  Hz, 1H; 5-H), 6.62 (dd,  $J = 8.39, 2.22$  Hz, 1H; 5'-H), 6.6 (d,  $J = 2.22$  Hz, 1H; 3'-H), 3.17 to 5.13 (m, 14H, sugar H).  $^{13}\text{C}$  NMR (100 MHz, methanol- $d_4$ ,  $\delta$ ): 192.58 (C=O), 163.59 (C-2'), 156.17 (C-4'), 149.91 (C4), 145.71 (C3), 144.86 (C $\beta$ ), 131.82 (C6'), 127.00 (C1), 125.87 (C6), 117.45 (C $\alpha$ ), 116.47 (C5), 116.10 (C5'), 115.07 (C1'), 108.05 (C2), 99.69 (C3'). MS (ESI,  $m/z$ ): 619 [ $\text{M} + \text{Na}$ ] $^+$ .

The available binding sites in isobutrin for metal are the two phenolic –OH groups and one carbonyl group C=O which is in conjugation with the double bond. But the sterically favored Ti binding site is at the hydroxyl group on ring B of isobutrin as shown in Figure 1.

## 3. RESULTS AND DISCUSSION

**3.1. Extraction and Structure Elucidation.** In this work we have extracted, isolated and characterized the isobutrin dye and studied its potential use as a sensitizer in DSSCs. We confirmed the structure of the extracted isobutrin by comparison of its physical constants and spectral properties ( $^1\text{H}$ ,  $^{13}\text{C}$  NMR and Mass Spectroscopy) with those reported in the literature,<sup>28</sup> as shown in Figure 1 and discussed in Experimental Section. The available binding sites in isobutrin for Ti are the two phenolic –OH groups and one carbonyl group C=O, which is in conjugation with the double bond. See the Supporting Information, S1.

**3.2. UV–Visible Spectroscopy.** From the UV–vis spectra of Figure 2A, it is seen that the  $\lambda_{\text{max}}$  for the juice and the purified isobutrin (bright yellow color as shown in inset) is at  $\sim 370$  nm.

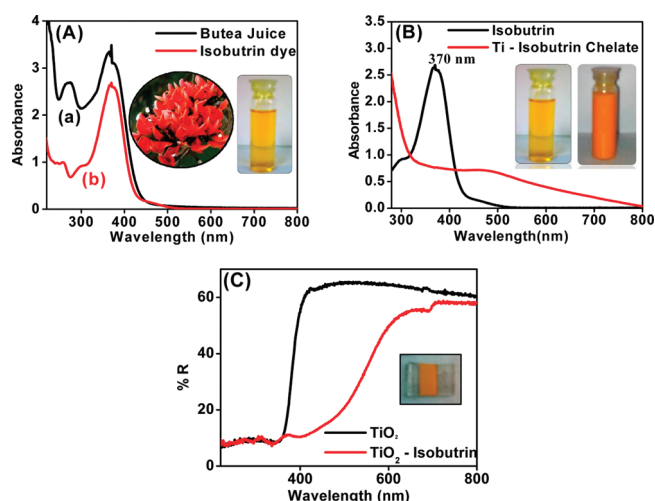


**Figure 2.** (A) UV-vis absorption spectra of butea juice and pure isobutrin, (B) UV-vis absorption spectra of pure isobutrin and Ti-isobutrin chelate, (C) diffuse reflectance spectra (DRS) of TiO<sub>2</sub> nanoparticle film and isobutrin dye-loaded TiO<sub>2</sub> film.

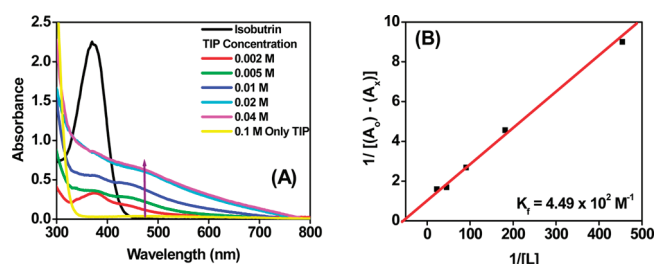


**Figure 3.** (A) UV-vis Spectra of Ti-isobutrin at various concentrations, (B) B-H plot of Ti-isobutrin chelate.

Because the absorption by isobutrin in the visible is only as an extended tail, one would think that this may not be effective for sensitization. However, we observed a very interesting aspect that its metal chelation shifts the absorption edge significantly toward the visible, as shown in Figure 2B. The diffuse reflectance spectra (DRS) of Figure 2C bear out the proposition showing significant absorption over the visible range from 400 to 650 nm.

According to Yoon et al.,<sup>29</sup> chelation of organic ligands with Ti (IV) ions can lead to strong dye-TiO<sub>2</sub> charge transfer (DTCT) bands in the visible region. This falls under the category of type II dyes where the electron injection occurs directly from the HOMO of the dye to the CB of TiO<sub>2</sub> by photoexcitation. The hydroxyl groups on the molecule bind strongly with TiO<sub>2</sub> giving rise to strong DTCT bands in the visible region. Similarly, in our work, we have observed that isobutrin forms a chelate with Ti (IV) ions through -OH group(s), because of which its optical absorption shows a significant shift toward orange. Indeed, after removal of TiO<sub>2</sub> films from this dye following the 24 h dye-loading process, its color changes to dark orange as shown in the inset of Figure 2C.

We examined the evolution of the UV-vis absorption spectra as a function of the concentration of Ti (while keeping the concentration of Isobutrin constant) to reveal the formation steps of Ti-isobutrin chelate. In this experiment, Titanium Tetra Iso-propoxide (TIP) of various concentration was added (0.002–0.04M)

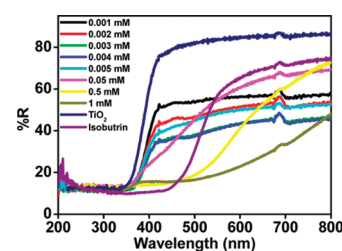


**Figure 4.** Diffuse reflectance spectra of Ti-isobutrin at various concentrations.

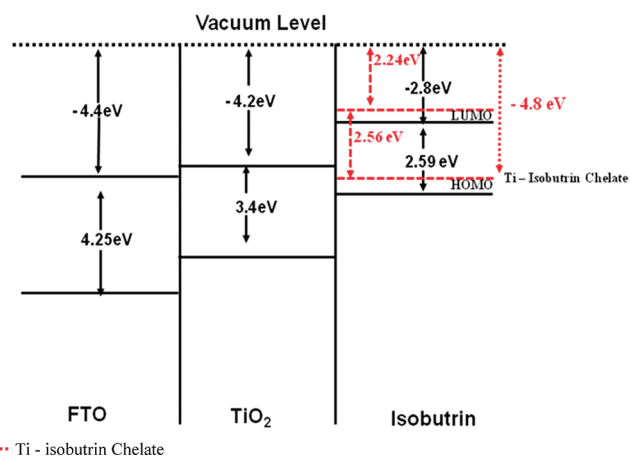


**Figure 5.** Band alignment of isobutrin dye with TiO<sub>2</sub>.

to 5 mM Isobutrin solution in methanol. UV-vis spectra of this solution were recorded and are presented in Figure 3A. From the graph, it is clear that the addition of Ti to Isobutrin progressively shifts the absorbance toward the visible region (peak near 480 nm). As the concentration of Ti is increased, the peak at 370 nm (attributed to Isobutrin) is seen to disappear even at small concentrations of Ti and the spectral weight appears to shift to the visible region.

The formation constant ( $K_f$ ) and its stability can be calculated using the B-H (Benesi-Hildebrand) plot.<sup>30,31</sup> Figure 3B shows the B-H plot for our case. From the graph the value of  $K_f$  is found to be  $\sim 4.49 \times 10^2 \text{ M}^{-1}$  which testifies to the ease of its formation from eq 1 in the Supporting Information, S2.

In order to explore the isobutrin-TiO<sub>2</sub> interaction further, we studied diffuse reflectance spectra (DRS) of the chelate with respect to concentration as shown in Figure 4.

Here the concentration of isobutrin was varied keeping the concentration of TiO<sub>2</sub> constant. From the DRS data it is seen that as the concentration of Isobutrin is increased from 0.001 mM to 1 mM the characteristic band of TiO<sub>2</sub> is modified due to chelation of isobutrin with Ti. The UV absorbing TiO<sub>2</sub> now shows prominent absorption in the visible region for the conjugate and this absorption goes on increasing with the concentration of Isobutrin until it reaches saturation at  $\sim 0.5$  mM (see the Supporting Information, S3).

**2.2. Band Alignment of Isobutrin with TiO<sub>2</sub>.** Figure 5 shows the results of HOMO-LUMO alignment of Ti-isobutrin chelate and pure isobutrin dye as calculated from cyclic voltammetry. It is found that the HOMO of Ti-isobutrin chelate is at  $-4.8$  eV and that of pure isobutrin dye is at  $-5.4$  eV with reference to the

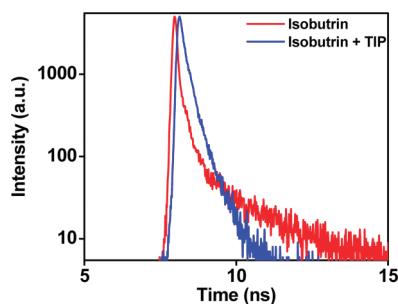


Figure 6. Fluorescence lifetime measurement of isobutrin and Ti-isobutrin chelate.

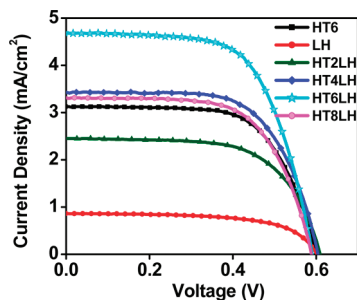


Figure 7. Solar cell characteristics for the case of anatase TiO<sub>2</sub> nanoparticle + light harvesting layer.

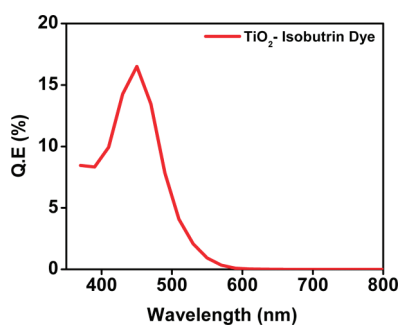


Figure 8. IPCE measurement of isobutrin dye-loaded TiO<sub>2</sub> film.

vacuum level. Thus after chelate formation the HOMO of isobutrin has shifted by 0.6 eV toward the positive side. This gave us an insight of the electron transfer process occurring in this isobutrin natural dye-sensitized solar cell.

**2.3. Fluorescence Lifetime Measurements.** To monitor the charge-transfer (CT) process in the isobutrin-TiO<sub>2</sub> system, we performed fluorescence lifetime measurements. These were carried out for isobutrin dye and Ti-isobutrin chelate in methanol and the data are shown in Figure 6. The samples were excited by a 440 nm diode laser (IBH, UK, NanoLED-440 L). The fluorescence signal of 550 nm was collected in magic angle using CP-PMT (Hamamatsu, Japan) detector. The Instrument response function is  $\sim 120$  ps. Photoluminescence (PL) results are included in the Supporting Information, S4.

It was found that chelation led to substantial quenching of the long lifetime component but the lifetime of the short lifetime component was seen to have increased. The  $\tau_1$  value for isobutrin was found to be 0.04 ns, while that for the chelate case to be 0.095

Table 1. Solar Cell Characteristic of Isobutrin Dye

name	$V_{oc}$ (V)	$J_{sc}$ (mA/cm <sup>2</sup> )	FF (%)	$\eta$ (%)
HT6	0.6	3.12	65.58	1.2
LH	0.6	0.86	62.27	0.32
HT2LH	0.6	2.44	63.8	0.95
HT4LH	0.6	3.42	64.79	1.3
HT6LH	0.58	4.67	64.14	1.8
HT8LH	0.59	3.31	64.41	1.3

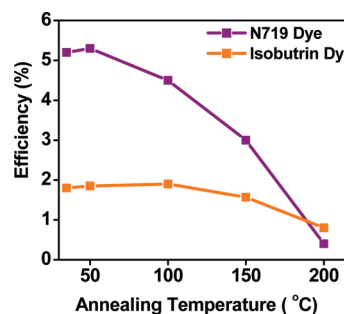


Figure 9. Solar conversion efficiency with respect to cell processing temperature.

ns. This change can be attributed to the conformational changes taking place in isobutrin during chelation and related hybridization changes. These observations are a testimony to the fact that chelation influences the electronics states and the attendant optical effects significantly. More work is clearly needed to elucidate these matters further.

**2.4. IV Characterization.** Figure 7 shows the  $I-V$  data for the case of anatase TiO<sub>2</sub> nanoparticle films using pure isobutrin dye. Here, light harvesting (LH) architecture was used. Wherein a highly transparent (HT) TiO<sub>2</sub> layer of thickness varying from 2 to 6 micrometers was used as a bottom layer followed by a light harvesting layer of TiO<sub>2</sub> spheres of thickness  $\sim 6$   $\mu$ m (each sphere of diameter around 400 nm). Table 1 shows the data for various thickness values of the bottom layer with constant thickness of LH layer. The optimum thickness of HT was found to be 6  $\mu$ m, which gave short circuit current density of 3.12 mA/cm<sup>2</sup> and open circuit voltage of 0.6 V, which gave efficiency of 1.2%. By using LH layer of 6  $\mu$ m thickness over this optimized thickness of HT layer, current density increased to 4.67 mA/cm<sup>2</sup>, which gave a conversion efficiency of 1.8%. Also, the  $I-V$  data for the case of anatase TiO<sub>2</sub> nanoparticle films using isobutrin dye at different stages of purification was studied as shown in the Supporting Information, S5.

**2.5. IPCE Measurement.** Figure 8 shows the IPCE spectra as a function of the wavelength for TiO<sub>2</sub> sensitized with isobutrin. It was calculated from the equation

$$\text{IPCE}(\%) = 1240 J_{sc} / \lambda P_{in}$$

where  $J_{sc}$  is the short-circuit current density,  $\lambda$  is the wavelength of the incident light, and  $P_{in}$  is the power of the incident light.

The absolute IPCE is seen to peak at 450 nm, which is in good agreement with the optical absorption of isobutrin dye chelated with Ti (IV) as mentioned earlier. The peaking of IPCE in the visible (with decrease toward higher energy photons) reflects the modified density of states due to chelating.

**2.6. Thermal Stability.** Before concluding, it is interesting to mention that the Ti-chelate system was found to be thermally quite stable as shown in Figure 9. In fact, we compared the stability of the solar cell efficiency upon annealing the cells at different temperatures and measuring the efficiency at room temperature. We found that the isobutrin-based cell efficiency began to degrade only after annealing the cells above 100 °C, whereas the efficiency of cells with N719 dye was found to start decreasing for annealing above 50 °C.

### 3. CONCLUSION

In summary, a new natural (metal free) sensitizer belonging to chalcone class, namely isobutrin, is extracted from a natural flower source *Butea Monosperma* (Flame of the Forest) for possible use in dye sensitized solar cells as well as other optoelectronic applications. In DSSCs, purified isobutrin yields very promising solar conversion efficiency of 1.8%. Interestingly the chelation of isobutrin to Ti shifts the optical absorption toward the visible (orange) making it effective in the DSSC operation. The formation constant of this chelate is found using B–H plot, which brings out the ease of its formation. The band alignment of this chelate is established using cyclic voltametry.

### ■ ASSOCIATED CONTENT

**S Supporting Information.** Additional characterization of isobutrin dye, which includes FTIR, PL, equation for calculation of  $K_f$ , concentration vs absorbance study, IV data with respect to purity of dye, and experimental details of thermal stability. This material is available free of charge via the Internet at <http://pubs.acs.org/>.

### ■ AUTHOR INFORMATION

#### Corresponding Author

\*Tel.: +91-20-25902260. Fax: +91-20-25902636. E-mail: sb.ogale@ncl.res.in or satishogale@gmail.com (S.B.O.); shruti.agar-kar28@gmail.com (S.A.); sp.joshi@ncl.res.in (S.P.J.).

### ■ ACKNOWLEDGMENT

S.A., V.D., and S.B.O. gratefully acknowledge funding from the Department of Information Technology, Government of India (Dr. K. Kumar and Dr. S. Chatterjee). S.J., R.K., and A.C. acknowledge in-house funding by NCL, CSIR, Pune, India. The authors will like to thank Dr. K. Krishnamoorthy for cyclic voltametry measurement/analysis and Abhigyan Sengupta and Rahul Khade for help with fluorescence lifetime measurements.

### ■ REFERENCES

- (1) Argazzi, R.; Murakami Iha, N. Y.; Zabri, H.; Odobel, F.; Bignozzi, C. A. *Coord. Chem. Rev.* **2004**, *248*, 1299–1316.
- (2) Calogero, G.; Marco, G. D.; Caramori, S.; Cazzanti, S.; Argazzi, R.; Bignozzi, C. A. *Energy Environ. Sci.* **2009**, *2*, 1162–1172.
- (3) Kyaw, A. K. K.; Sun, X. W.; Zhao, J. L.; Wang, J. X.; Zhao, D. W.; Wei, X. F.; Liu, X. W.; Demir, H. V.; Wu, T. J. *Phys. D: Appl. Phys.* **2011**, *44*, 045102.
- (4) Robertson, N. *Angew. Chem., Int. Ed.* **2006**, *45*, 2338–2345.
- (5) O'Regan, B.; Grätzel, M. *Nature* **1991**, *353*, 737–740.
- (6) Nazeeruddin, M. K.; Kay, A.; Rodicio, I.; Humphry-Baker, R.; Muller, E.; Vlachopoulos, N.; Grätzel, M. J. *Am. Chem. Soc.* **1993**, *115*, 6382–6390.

- (7) Sauvage, F.; Fischer, M. K. R.; Mishra, A.; Zakeeruddin, S. M.; Nazeeruddin, M. K.; Bauerle, P.; Grätzel, M. *ChemSusChem* **2009**, *2*, 761–768.
- (8) Amao, Y.; Komori, T. *Biosens. Bioelectron.* **2004**, *19*, 843–847.
- (9) Wongcharee, K.; Meeyoo, V.; Chavadej, S. *Sol. Energy Mater. Sol. Cells* **2006**, *11*, 566–572.
- (10) Dai, Q.; Rabani, J. *Chem. Commun.* **2001**, 2142–2143.
- (11) Polo, A.; Yukie, N.; Iha, M. *Sol. Energy Mater. Sol. Cells* **2006**, *90*, 1936–1944.
- (12) Garcia, C.; Polo, A.; Yukie, N.; Iha, M. *J. Photochem. Photobiol.* **2003**, *160*, 81–91.
- (13) Kay, A.; Humphry-Baker, R.; Grätzel, M. *J. Phys. Chem.* **1994**, *98*, 952–959.
- (14) Kamat, P. V.; Chauvet, J.-P.; Fessenden, R. W. *J. Phys. Chem.* **1986**, *90*, 1389–1394.
- (15) Amao, Y.; Yamada, Y.; Aoki, K. *J. Photochem. Photobiol. A: Chem.* **2004**, *164*, 47–51.
- (16) Ito, S.; Saitou, T.; Imahori, H.; Ueharad, H.; Hasegawa, N. *Energy Environ. Sci.* **2010**, *3*, 905–909.
- (17) Simiyu, J.; Adula, B. O.; Mwabora, J. M. *Prog. Colloid Polym. Sci.* **2004**, *125*, 34–37.
- (18) Bakowska, A.; Kucharska, A. Z.; Oszmianski, J. *Food Chem.* **2003**, *81*, 349.
- (19) Hao, S.; Wu, J.; Fan, L.; Huang, Y.; Lin, J.; Wei, Y. *Sol. Energy Mater. Sol. Cells* **2004**, *76*, 745–750.
- (20) Rubinskiene, M.; Viskelis, P.; Jasutiene, I.; Viskeliene, R.; Bobunas, C. *Food Res. Int.* **2005**, *38*, 867.
- (21) Adams, J. B. *J. Sci. Food Agri.* **1973**, *24*, 747–762.
- (22) Campbell, W. M.; Jolley, K. W.; Wagner, P.; Wagner, K.; Walsh, P. J.; Gordon, K. C.; S-Mende, L.; Nazeeruddin, M. K.; Wang, Q.; Grätzel, M.; Officer, D. L. *J. Phys. Chem. C* **2007**, *111*, 11760–11762.
- (23) Kumara, G. R. A.; Kaneko, S.; Okuya, M.; Onwona-Agyeman, B.; Konno, A.; Tennakone, K. *Sol. Energy Mater. Sol. Cells* **2006**, *90*, 1220–1226.
- (24) Zhang, D.; Lanier, S. M.; Downing, J. A.; Avent, J. L.; Lum, J.; McHale, J. L. *J. Photochem. Photobiol. A: Chem.* **2008**, *195*, 72–80.
- (25) Wang, X.-F.; Zhan, C.-H.; Maoka, T.; Wada, Y.; Koyama, Y. *Chem. Phys. Lett.* **2007**, *447*, 79–85.
- (26) Chen, D.; Cao, L.; Huang, F.; Imperia, P.; Cheng, Y.-B.; Caruso, R. A. *J. Am. Chem. Soc.* **2010**, *132*, 4438–4444.
- (27) Muduli, S.; Lee, W.; Dhas, V.; Mujawar, S.; Dubey, M.; Vijayamohan, K.; Han, S. H.; Ogale, S. *ACS Appl. Mater. Interfaces* **2009**, *1*, 2030–2035.
- (28) Saxena, A. K.; Gupta, B. D.; Kapahi, B. K.; Muthiah, S.; Mondhe, D. M.; Qazi, G. N.; Kumar, V.; Mathan, G. U.S. Patent 2006/0280817 A1.
- (29) Tae, E. L.; Lee, S. H.; Lee, J. K.; Yoo, S. S.; Kang, E. J.; Yoon, K. B. *J. Phys. Chem. B* **2005**, *109*, 22513–22522.
- (30) Benesi, H. A.; Hildebrand, J. H. *J. Am. Chem. Soc.* **1949**, *71*, 2703–2707.
- (31) Kim, D.; Shin, E. *Bull. Korean Chem. Soc.* **2003**, *24*, 1490–1495.